Gas-Holdup Measurements in Bubble Columns Using Computed Tomography

Sailesh B. Kumar, Davood Moslemian, and Milorad P. Duduković
Chemical Reaction Engineering Laboratory, Dept. of Chemical Engineering, Washington University, St. Louis, MO 63130

A computed tomographic scanner was developed for imaging gas-holdup distributions in two-phase flow systems such as bubble columns and fluidized beds. The scanner has been used to study the effects of various operating parameters (such as column diameter, superficial gas velocity, and distributor type) on the gas holdup and its distribution in an air–water bubble column. The experimental investigation shows that the column dimensions have no significant effect on the void fraction when the column diameter is greater than 0.15 m. Differences in the holdup distribution due to the kind of distributor used are significant only at low gas flow rates. Surface tension of the liquid has a profound influence on the gas holdup and its distribution.

Introduction

Bubble columns are used in the chemical and process industry as contactors for mass-transfer processes and chemical reaction between gases and liquids. Owing to the complexity of the two-phase flow pattern a thorough understanding of the hydrodynamics involved has not been achieved. Among the various hydrodynamic parameters of special interest is the holdup distribution of the gaseous phase, as it affects other transport processes and thus the overall reactor performance. Gas holdup is important in the determination of the overall residence time of the gas as well as the pressure drop in the system. It is also a measure of the interfacial area available for phase interactions, and its spatial distribution affects the phase recirculation (back mixing) in the bubble column. Since heat, mass, and momentum transfer depend on these quantities, gas holdup and its distribution constitute important design parameters for any multiphase flow system.

Although the void fraction, or the gas holdup has been the subject of extensive experimental research, a review of the literature reveals that the reported measurements have been predominantly global in nature, that is, mainly the overall gas holdup in the vessel has been reported and extensive investigations of the local holdup and its spatial distribution are not available. One of the reasons for this has been the lack of experimental techniques that are capable of making local measurements over the whole vessel without an extensive and intrusive data-collection process. At the Chemical Reaction Engineering Laboratory (CREL) a computed tomographic (CT) scanner has been developed for imaging-phase-holdup distribution in two-phase flow systems such as bubble columns and fluidized beds. The scanner is a versatile instrument that enables the quantification of the time-averaged holdup distribution for two-phase flows under a wide range of operating conditions. The measurements can be made at different distances above the distributor for flows in test sections up to 0.35 m diameter. This allows the quantification of the effects of operating conditions on the gas-holdup distribution in a bubble column.

Computed Tomographic Scanner

The tomographic scanner at CREL uses the third-generation scanning configuration, in which an array of collimated detectors are arranged in an arc at the center of which is the source of radiation. The whole assembly of the detectors and the radiation source are mounted on a gantry that is capable of being rotated about the axis of the test section through a stepper motor interfaced to a host computer. The source used is an encapsulated 100-mCi cesium-137 isotope. The encapsulation is such that it provides a fan beam subtending an angle of 40° in the horizontal plane. The source has been further collimated using a $0.2 \times 0.1 \times 0.1$-m lead brick with a central slit such that the emerging beam has a thickness of 6.5 mm at a distance of 0.28 m from the source. The detectors used are 2 in. × 2 in. (51 mm × 51 mm) NaI scintilla-

Correspondence concerning this article should be addressed to M. P. Duduković.
Present address of: S. B. Kumar, UOP, Riverside, IL; D. Moslemian, Department of Mechanical Engineering, Florida Atlantic University, Boca Raton, FL.

tion detectors because these were readily available from our Computer Automated Radioactive Particle Tracking (CARPT) facility (Devanathan et al., 1990; Yang et al., 1993). In order to be able to scan columns up to 0.35 m in diameter the arc radius of the detectors was 0.923 m. With this radius, only eleven detectors could be accommodated in the fan beam arc of 40°. In order to increase the number of projection measurements in one view of the column, the number of detectors in the arc was effectively increased by using a collimator that moves across the detector arc. By this method the detectors were made to sample multiple rays. However, this increases the scan time (the scan time increases in proportion to the number of additional rays sampled by a detector). The movement of the collimator is achieved by another independent stepper motor, also interfaced with the host computer. The collimator made of lead is 6.35 cm deep and has a height of 7.62 cm, so that the detectors are completely shielded by the collimator. It also has rectangular holes 5×10 mm at locations appropriate to each of the detectors for sampling the beams. These dimensions for the collimator holes were optimized based on considerations of providing adequate area for detecting photons with good statistics in the chosen sampling period.

The spatial resolution that a scanner is capable of is a function of the detector aperture D_a, the focal-spot width (source size) s, and the magnification factor M defined as the ratio of source-detector distance to the source-object distance. A measure of the spatial resolution is the point-spread function (PSF), which specifies the extent to which a point object would be blurred in its image. Yester and Barnes (1977) provide the following simple relationship for the width of PSF:

$$\frac{1}{M}\sqrt{D_a^2 + (M-1)^2 s^2}.$$

For our case the detector aperture is 5 mm, the source is a sphere of 3-mm diameter and the average magnification factor is 1.5 (it varies with position in the imaged object). Thus, the average PSF for the present scanner works out to be 3.5 mm. However, the pixel size is conservatively set in the range of 5 to 6 mm. The spatial resolution in the vertical direction is the sampled beam thickness of 10 mm.

The entire scanning assembly weighs about 90 kg, and consequently the maximum rotational speed that can be achieved is about 1 rpm. The holdup distribution that can be obtained can therefore only be a time-averaged one. The scanning assembly has a central opening large enough for it to translate up and down with respect to the test section. This latter motion is achieved by means of four precision, square, threaded screws supporting the scanning assembly at the corners. They can be driven synchronously to accomplish the axial positioning required for scanning different horizontal sections of the column. The data-acquisition system has been discussed in Moslemian et al. (1993) and Kumar et al. (1995). Figure 1 shows the CT scanner.

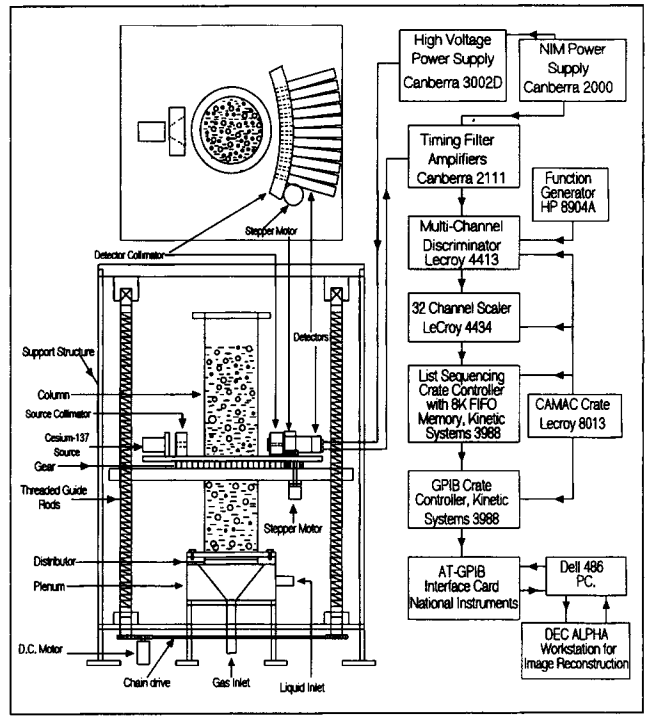

Figure 1. CT scanner.

Image Reconstruction Algorithm

There are numerous algorithms that are available for image reconstruction and there are software packages—Snark89 (Herman et al., 1989) and RECLBL Library (Huesman, 1977)—that have implemented most of these algorithms. In the field of medicine the algorithms that have found wide acceptance are the ones based on Fourier techniques or the ones referred to as the algebraic reconstruction technique (ART). For the system under discussion an algorithm based on maximum-likelihood principles is used. This algorithm referred to as the estimation-maximization (E-M) algorithm has found wider acceptance in emission tomography. It is based on an exact stochastic model of the projection measurements, and is an iterative algebraic technique that finds the maximum-likelihood estimate of the image. The measured projections are considered to be incomplete data in the sense that no measurement is completely representative of the system being investigated. Two sample spaces X and Y are defined with the observed incomplete data $y \subseteq Y$ having a probability density function $g(y, \theta)$ (either known or assumed), where θ is a vector of parameters to be estimated. The data that one would ideally obtain are referred to as complete data $x \subseteq X$ and are related to y through a mapping $h: X \rightarrow Y$ such that $h(x) = y$. The postulate is that the incomplete data are a subset of the complete (unobserved) data. The criteria for defining the complete data space are based on the physics of the problem. If x has a probability density function $f(x, \theta)$, then

$$g(y, \theta) = \int_{\{x:h(x)=y\}} f(x, \theta)\, dx, \tag{1}$$

x being determined by $y = y(x)$.

The E-M algorithm aims at finding θ, which maximizes $g(y, \theta)$ using the density function $f(x, \theta)$. The E step consists of forming the conditional expectation $E(\ln f(x, \theta) \mid y, \theta^n)$, where θ^n represents the current estimate of the vector of parameters. The M step chooses θ^{n+1} as the new vector es-

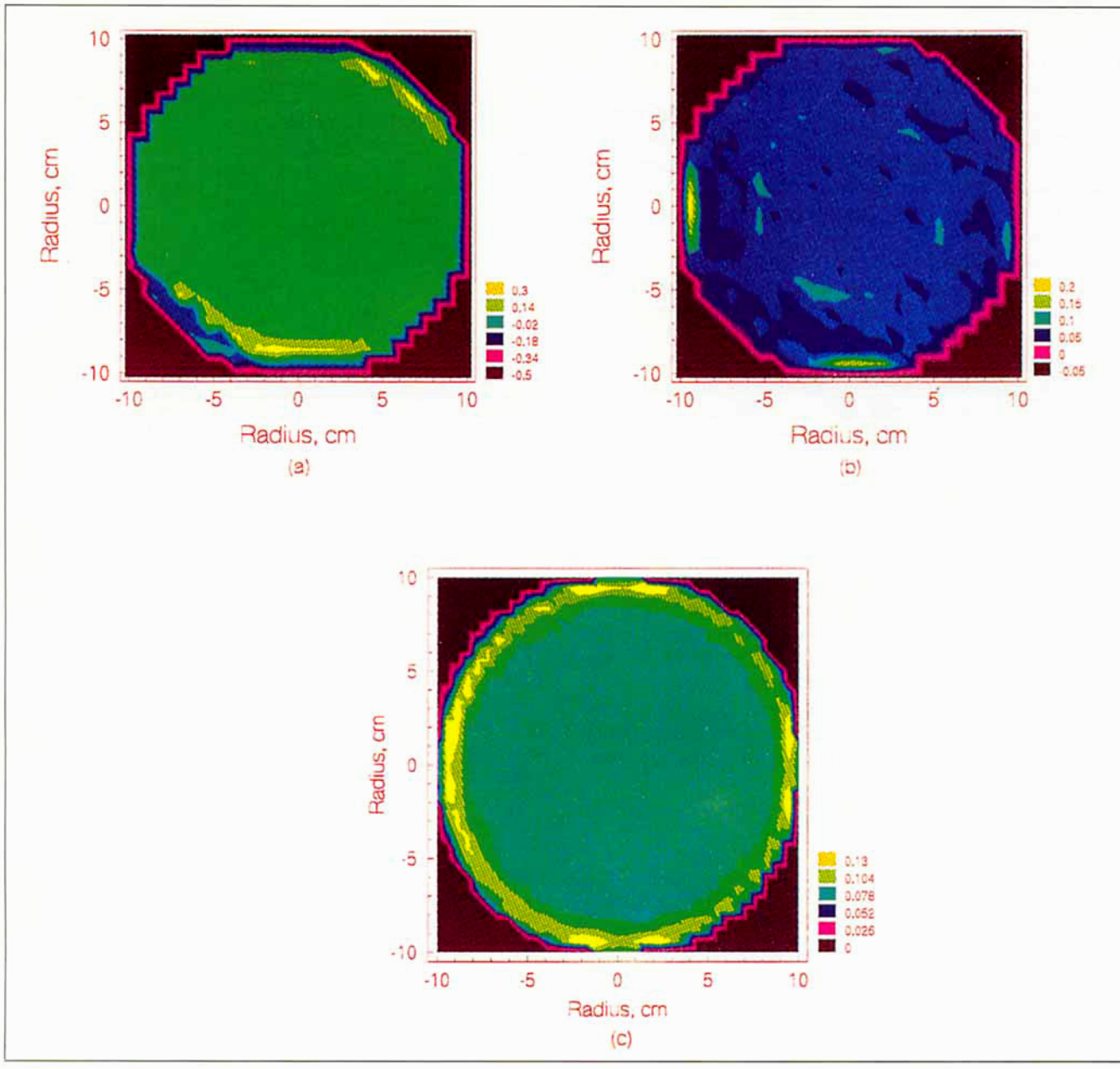

Figure 2. Reconstruction from different algorithms: (a) convolution-backprojection; (b) ART; (c) E-M algorithm.

timate that maximizes the conditional expectation. The new estimate is then used in the E step and the process is repeated until the logarithm of the likelihood function, $\ln g(y, \theta)$ is maximized. A comprehensive article on the algorithm has been presented by Dempster et al. (1977).

Some of the merits of this algorithm are that it can account for statistical variations, and can easily incorporate effects of nonuniform beams and other pathological effects. There is also no need for interpolating and rearranging (rebinning) the fan beam data into parallel beams and it assures the nonnegativity of the final reconstruction. Details of the adaptation of the algorithm for transmission tomography can be found in Lange and Carson (1984).

Comparison between the reconstructions obtained by the E-M algorithm over the reconstructions of other well-known algorithms for some test phantoms (known density distribution) is now illustrated. The transmission data (ratio of I/I_0) for a plexiglass column 20.32 cm in diameter filled with water was acquired over 90 views with 39 projections each. The image was reconstructed via the Snark89 image-reconstruction package using the convolution method for divergent beam projection data (Herman et al., 1989) as well as by an additive ART algorithm (Herman et al., 1989). These are compared with the image reconstructed by the E-M algorithm in Figure 2. The reconstructed number in each pixel should ideally be 0.086 cm^2/g, corresponding to the mass-attenuation coefficient of water at 660 keV, the peak energy of the radiations from Cs-137. Although visually the reconstruction by the convolution method appears to be better, the comparison between the reconstructions has to be made on the basis of the

Table 1. Mean and Standard Deviation of Attenuation Coefficients Reconstructed by Three Algorithms

Algorithm	Reconst. Mean	Std. Dev.
Convolution	0.0736	0.060
ART	0.0728	0.030
E-M Algorithm	0.0887	0.003

magnitudes assigned to the color bar. The mean attenuation coefficient and the deviation from the mean obtained using the three algorithms are reported in Table 1. The mean reconstructed value obtained using the traditionally used algorithms are far away from the desired value of 0.086 cm^2/g, and the spread in the pixel values is much larger. The uniformity of the reconstruction by the E-M algorithm can be judged on the basis of the corresponding numbers in the table.

Holdup Measurements: Tomography vs. Other Techniques

In the literature it can be seen that radiation techniques have served as the reference for calibration of holdup measurements made by other techniques (Sim and Lahey, 1986). This can be attributed to the noninvasive nature of the method. In the present study the cross-sectional mean gas holdup computed from the two-dimensional distribution is compared with the gas-holdup measurements obtained by using the pressure-drop method as well as with the overall gas holdup obtained using the bed-expansion method. The pressure drop between two sections approximately 0.2 m apart in a 0.14-m diameter column was measured using a simple manometer with water as the measuring fluid. The gas holdup in between the two sections was then computed on the basis of the expression

$$\frac{dP}{dZ} = -\rho_l g(1-\epsilon). \tag{2}$$

Use of the preceding expression implies that the effects of liquid acceleration and wall friction can be neglected. A tomographic scan was made halfway between the two pressure taps. The cross-sectional mean gas holdup was computed from the two-dimensional distribution of the gas holdup by first circumferentially averaging the data and then using the following expression:

$$\bar{\epsilon} = \frac{2}{R^2}\int_0^R \epsilon(r) r\, dr, \tag{3}$$

where R is the column radius. Table 2 compares the results for different gas velocities. Also listed in the table are the corresponding overall gas holdups obtained using the bed-expansion method. Considering that the resolution of the scale on the manometer was approximately 1 mm, the measurements from the scanner can be considered to compare well with the other methods.

Table 2. Comparison of Tomographic Results with Pressure Drop Measurements

Sup. Gas Vel. U_g, m/s	Void Fraction		
	CT	ΔP	Bed Expansion
0.02	0.087	0.088	0.085
0.05	0.123	0.125	0.129
0.08	0.147	0.150	0.144
0.12	0.179	0.182	0.188

Reproducibility of CT Measurements

The measurements for the gas holdup distribution in a 0.44-m diameter column were repeated on two successive days for demonstrating the reproducibility of the experimental measurements. The gas was introduced through a perforated-plate distributor with an effective open area of 0.06% (253 holes of 0.7-mm diameter arranged on 11 concentric circles). The experiments were repeated at two superficial gas velocities: 0.02 and 0.05 m/s. The cross-sectional distribution of the gas holdup was approximately axisymmetric and the reproducibility is illustrated by comparing the azimuthally averaged radial variation of gas holdup. Figures 3a and 3b show this comparison for the superficial gas velocities of 0.02 m/s and 0.05 m/s, respectively. These results correspond to the axial location of 0.8 m from the distributor where the end effects are minimal. In both cases similar magnitudes of the gas holdup are obtained at most of the radial locations. However, at the gas velocity of 0.02 m/s the plot appears to show a greater difference in the gas holdup for the two repeat runs in the region close to the center of the column. The percentage difference between the two runs (based on the first run) at the center (where the difference is maximum) is approximately 9%. The differences in the results cannot be wholly attributed to the lack of precision of the CT measurement, since differences in flow characteristics are expected between repeated multiphase flow runs. One cause for such differences is the nature of the surfactants contained in water that affect the bubble sizes and in turn the gas holdup. These effects are more pronounced at low gas velocities.

Comparison of CT Results with Results in the Literature

For the purpose of comparing the CT measurements with well-known results in the literature, the flow conditions of Hills (1974), were replicated. The column internal diameter was 0.139 m and the distributor used was a perforated plate

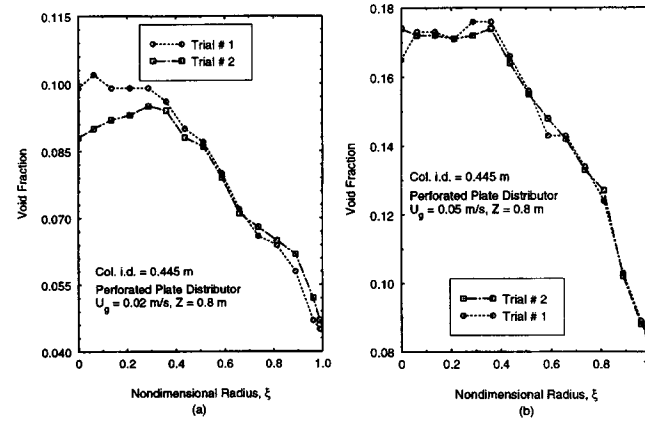

Figure 3. Reproducibility of CT measurements for gas holdup.

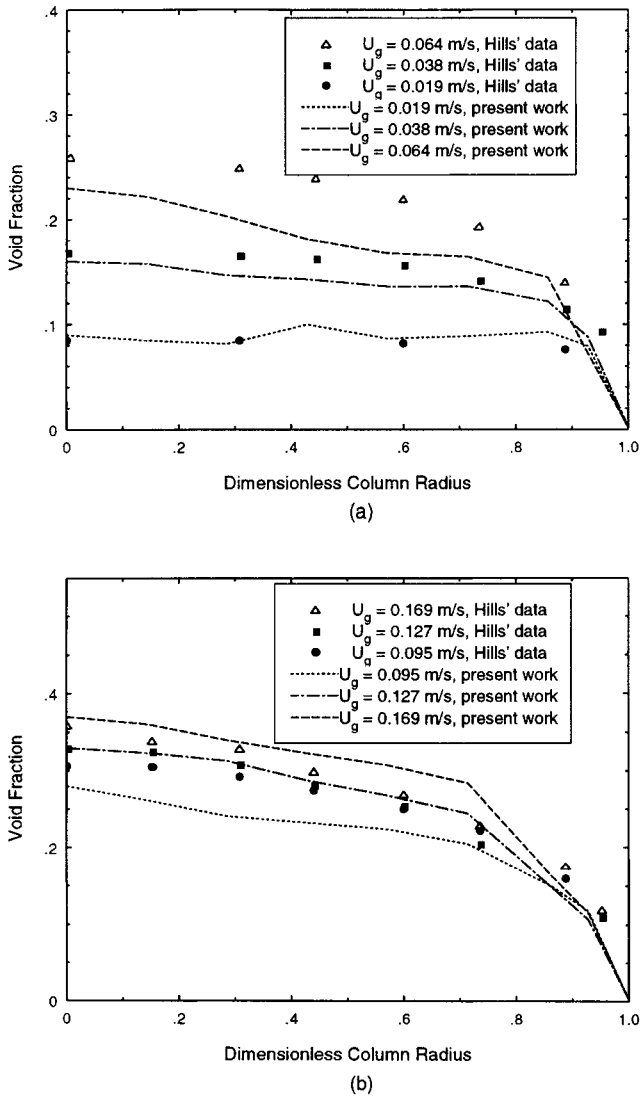

Figure 4. Measured gas holdup profiles in a bubble column under the experimental conditions of Hills (1974).

(Plate B of Hills) having 61 holes 0.4 mm in diameter (1 central, the rest uniformly spaced on three circles). The static liquid height used was 1.07 m (Hills does not state the L/D ratio used in his work). The scan was made at 0.6 m above the distributor, and the superficial gas velocities were matched to those used by Hills. Regular tap water provided by the St. Louis County Water Co. was used as the liquid phase. Filtered and dehumidified air was used for the gas phase. From the two-dimensional distribution of mass attenuation coefficients provided by the CT scan, the gas-holdup profiles are extracted by comparing the image pixel-by-pixel to the corresponding image obtained for the static column (no gas bubbling). The distribution obtained is close to being axisymmetric, and so the gas-holdup profiles presented in Figures 4a and 4b are all circumferentially averaged. Also plotted are the experimental data obtained by Hills. The data have been presented in two plots, primarily to reduce the density of plotted points. The gas holdup obtained currently compares well with Hills' data at low and high gas velocities,

Table 3. Comparison of Cross-Sectional Average and Overall Gas Holdup

Sup. Gas Vel. U_g, m/s	Bed Expansion cm	Overall Gas Holdup	Cross-Sectional Avg. Void Fraction
0.019	9.3	0.082	0.077
0.038	14.0	0.114	0.104
0.064	16.0	0.133	0.132
0.095	21.5	0.167	0.176
0.127	26.0	0.200	0.200
0.169	30.0	0.223	0.230

corresponding to the bubbly and churn-turbulent flow regimes. At the intermediate velocities (the transition regime) the measured holdup is lower than that of Hills. In addition, the profiles (at all the velocities) are much flatter. It has to be noted that with Hills' data the effect of superficial gas velocity on the gas holdup is high in the lower range of velocities and small at the higher velocities. In contrast the present data exhibit an approximately uniform trend in the way the gas velocity affects the gas holdup. Therefore, it appears that in spite of matching all the experimental conditions, the flow has not been reproduced. The lack of reproducibility of air–water two-phase flow data is not a new phenomenon, since the presence of surfactants in even trace amounts in water can affect the flow behavior. The gas-holdup results from scanning, however, can be verified on the basis of the comparison between the cross-sectionally averaged gas holdup with the overall holdup obtained by the bed expansion method as shown in Table 3.

Operating Conditions for Gas-Holdup Measurements in Bubble Columns

Experiments were performed in bubble columns of five diameters (0.102, 0.14, 0.19, 0.26 and 0.30 m) using air and mainly tap water as the gas and liquid phase, respectively. For assessing the effect of liquid properties some experimental runs were made with deionized water as well as a 50% isopropanol–water mixture as the liquid phase. Four superficial gas velocities (0.02, 0.05, 0.08 and 0.12 m/s) were used for most of the columns. For the two largest of the five columns the maximum superficial gas velocity used was 0.10 m/s instead of 0.12 m/s due to large bed expansions and the consequent nonavailability of free expansion space in the columns, and also due to the excessively turbulent nature of the flow at higher gas flow rates. These velocities cover all the flow regimes from bubble to churn turbulent in all the columns. For all the column sizes the experiments were conducted with a static liquid height to diameter ratio of at least 5. This is the recommended ratio in order for the effects of the bed height to be negligible on the flow properties (Wilkinson et al., 1992). However, a few other ratios were also used to evaluate the effect of the static liquid height on the gas holdup and its distribution. All the runs were made with zero liquid superficial velocity (i.e., no net liquid flow). The data were obtained mainly in columns fitted with a perforated-plate distributor. The distributors were made out of 0.0032-m-thick aluminum plates. The characteristics of the hole patterns and their sizes for the different columns are listed in Table 4. To evaluate the effects of gas distribution,

Table 4. Characteristics of Perforated Plates Used as Distributors

Col. Dia. m	Distributor Characteristics: No. of Holes, Hole Dia., mm	Pattern	Porosity, %
0.10	95, 0.5	Triangular pitch of 0.9 cm	0.23
0.14	61, 0.4	On 3 concentric circles 1.5 cm apart	0.05
0.19	156, 0.5	Square pitch of 1.25 cm	0.10
0.26	193, 0.4	On 8 concentric circles 1.5 cm apart	0.05
0.30	181, 0.7	On 9 concentric circles 1.5 cm apart	0.10

the flow in the 0.19-m-diameter bubble column was imaged with two other types of gas distributors, in addition to the perforated plate. The two other distributors were a simple cone and a single bubble cap riser. For most of the runs the scans were performed at five different elevations above the distributor for capturing the evolution of holdup distribution with axial position. While the intermediate levels for the scans for all the columns were identical, the levels for the scans at the ends (close to the distributor and the free surface) varied from column to column, depending on the accessibility for the scanning assembly and on bed expansion.

Experimental Results and Discussion

Gas holdup is linked with bubble sizes, their distribution, and their frequency. These parameters are dependent on the flow regime, and render the gas holdup a function of the flow rates of the gas and the liquid phases and the dimensions of the flow section. The formation size of the bubbles and their subsequent coalescence or breakup also affect gas holdup and, hence, influences of the gas distributor and surfactant concentration in the liquid phase are to be expected. The bubble-size distribution is a function of the liquid viscosity, and therefore gas holdup also depends on liquid viscosity. The bubble formation process and the physiochemical properties are dependent on the pressure and temperature in the system. In addition, effects of gas density (Wilkinson and Dierendonck, 1990; Clark, 1990), elastic properties of the liquid phase (Kelkar and Shah, 1985; Kawase and Moo-Young, 1986), the aspect ratio of the system (Reilly et al., 1986; Wilkinson et al., 1992), the molecular structure of the phases (Kelkar et al., 1983), the column inclination (Yamashita, 1985) and even the startup procedures (Prakash and Briens, 1990) have been reported to influence gas holdup. The objective of our experimental program was to evaluate the effects of some of the preceding operating parameters on gas holdup and its distribution. The parameters considered were column diameter, superficial gas velocity, type of distributor, the ratio of static liquid height to the column diameter, and some limited variations in the liquid properties. In what follows, the results of this investigation are presented.

Effect of column diameter

Based on a large number of experimental studies Shah et al. (1982) and Reilly et al. (1986) concluded that for columns with diameter larger than 0.15 m, column size has no effect on the overall gas holdup. In general it is now accepted that the holdup measured in columns with at least this diameter is

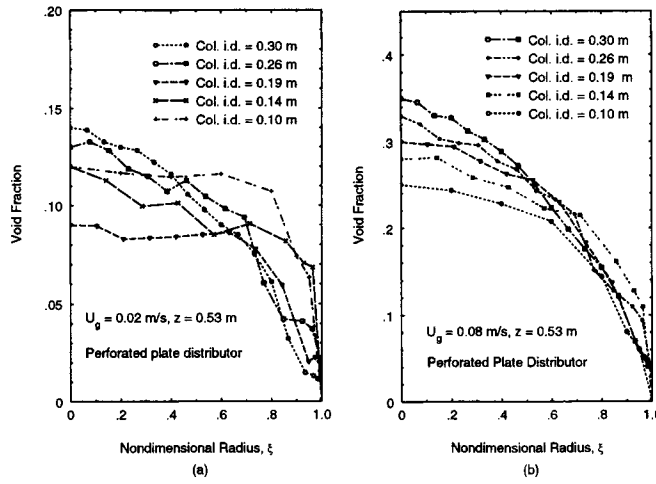

Figure 5. Effect of column diameter on the measured gas-holdup profile: (a) U_g = 0.02 m/s; (b) U_g = 0.08 m/s.

representative of data for which the effects of column dimensions can be neglected. Based on their study of large-diameter bubble columns, Koide et al. (1979) claim that the radial distribution of the gas holdup is flatter than that in a small column. For gas–liquid flow in small-diameter conduits such as pipes (1 to 2 in. in diameter) there is now a lot of data to suggest that the gas-holdup profile is saddle-shaped with the peaks at the walls especially at low flow rates (Malnes, 1966; Serizawa et al., 1975; Wang et al., 1987). Such saddle-shaped profiles have not been observed in larger-diameter vessels such as bubble columns, and it can be assumed that they are the result of wall effects. In bubble columns the void fraction distribution is parabolic at high gas flow rates and tend to become flatter at lower gas flow rates. These general observations in the literature have been confirmed by our experimental results.

The effect of column diameter on the gas-holdup distribution is shown in Figures 5a and 5b for superficial gas velocities corresponding to flow in the bubbly and churn-turbulent flow regimes, respectively. The gas-holdup profiles are from the scans of the columns at a section where end effects are negligible. At the low gas flow rate (U_g = 0.02 m/s), it is evident that the column diameter has some influence on the gas holdup, although there appears to be no specific trend to this effect. At the gas flow rate corresponding to U_g = 0.08 m/s, there is a continuous increase in the gas holdup with column diameter. The integral area under the curves was computed to evaluate the cross-sectional mean gas holdup, and are tabulated in Table 5. At the low gas velocity the cross-sectional

Table 5. Cross-sectional Mean Void Fraction as a Function of Column Diameter

Column Dia. m	X-Sect. Mean Void Fraction: U_g = 0.02 m/s	U_g = 0.08 m/s
0.10	0.106	0.191
0.14	0.094	0.209
0.19	0.075	0.225
0.26	0.095	0.234
0.30	0.104	0.238

Table 6. Power-Law Exponent as a Function of Column Diameter

Column Dia. m	Power-Law Exponent m	
	$U_g = 0.02$ m/s	$U_g = 0.08$ m/s
0.10	11.0	3.8
0.14	4.6	3.3
0.19	5.3	2.7
0.26	2.2	2.2
0.30	2.0	1.6

mean gas holdup decreases initially with the column diameter and then increases again. At the higher gas velocity the corresponding values continuously increase with the column diameter, although this increase tapers off gradually. This observation is in line with the observation made in the literature that the overall gas holdup is unaffected by the column diameter, provided it is greater than 0.15 m.

It is customary to describe the void-fraction profiles with a power-law expression (Miyauchi et al., 1981) of the type:

$$\epsilon(r) = \tilde{\epsilon}\left[1 - c\left(\frac{r}{R}\right)^m\right]\left(\frac{m+2}{m}\right), \qquad (4)$$

where $\tilde{\epsilon}$ is a parameter related to the cross-sectional mean gas holdup, m is the power-law exponent, and c is the parameter that accounts for the nonzero gas holdup observed close to the wall. The power-law exponent m provides a measure of the steepness or flatness of the gas-holdup profile. High values of m indicate a very flat distribution (uniform gas-holdup distribution across the section), and a decrease in the magnitude of m indicates the increasing tendency of the profiles to be parabolic. The exponent m for the conditions just discussed are tabulated in Table 6. The holdup profiles tend to be flat in smaller-diameter columns as well as at low superficial gas velocities, and are parabolic in larger columns as well as at higher gas flow rates. A measure of the fit of the power law (Eq. 4) to the experimental data in columns 0.10 m and 0.26 m in diameter is shown in Figures 6a and 6b.

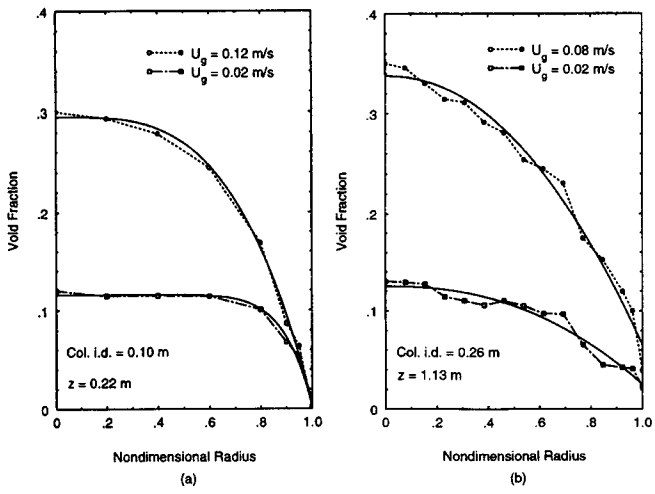

Figure 6. Power law fits to the measured gas-holdup profiles: col. ID (a) 0.10 m, (b) 0.26 m.

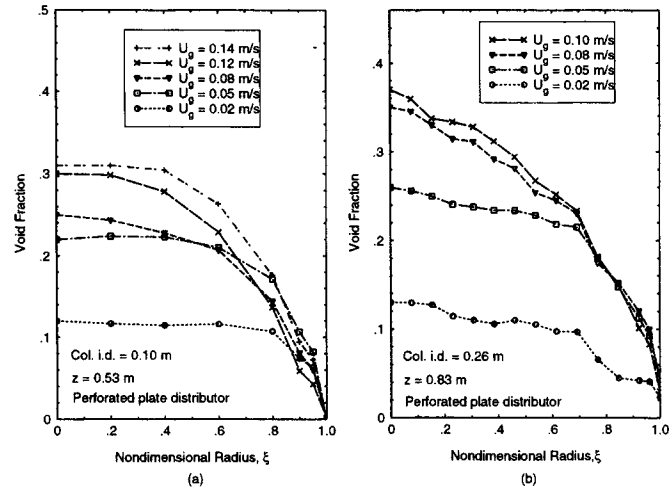

Figure 7. Effect of superficial gas velocity on the measured gas-holdup distribution: col. ID (a) 0.10 m, (b) 0.26 m.

Effect of superficial gas velocity

The effect of superficial gas velocity on the gas-holdup distribution is demonstrated in two of the columns studied. Figures 7a and 7b correspond to the gas-holdup distributions obtained in the 0.10-m- and 0.26-m-diameter columns as a function of superficial gas velocity. The data correspond to scans at one fixed axial location that is well away from entrance or free surface effects. In general, an increase in the gas velocity leads to an increase in the magnitude of the local gas holdup at all column radii except at regions close to the wall. The magnitude of this increase is much larger at the lower velocities corresponding to the bubbly and transition flow regimes. At the higher velocities (churn-turbulent flow), the increase is relatively smaller. The gas-holdup profile changes from a flatter distribution to a more parabolic one with increase in the superficial gas velocity. This conclusion is based on the values of the power-law exponent m tabulated in Table 7 for the two cases considered. In the smaller-diameter column, the value of the power-law exponent decreases with increase in the superficial gas velocity. For the larger column the exponent is relatively smaller and is approximately constant with increase in gas velocity. Thus, in relatively larger columns the power-law exponent that determines the profile of the radial distribution of the gas holdup is typically in the range of 2 to 2.5.

In the literature the measurements for the overall gas holdup are plotted as a function of superficial gas velocity and the variation is expressed using the following type of relationship:

Table 7. Power-Law Exponent as a Function of Superficial Gas Velocity

Sup. Gas Vel. U_g, m/s	Power-Law Exponent, m	
	Col. Dia. = 0.1 m	Col. Dia. = 0.26 m
0.02	11.0	2.3
0.05	6.7	2.3
0.08	3.8	2.2
0.12	2.7	2.1

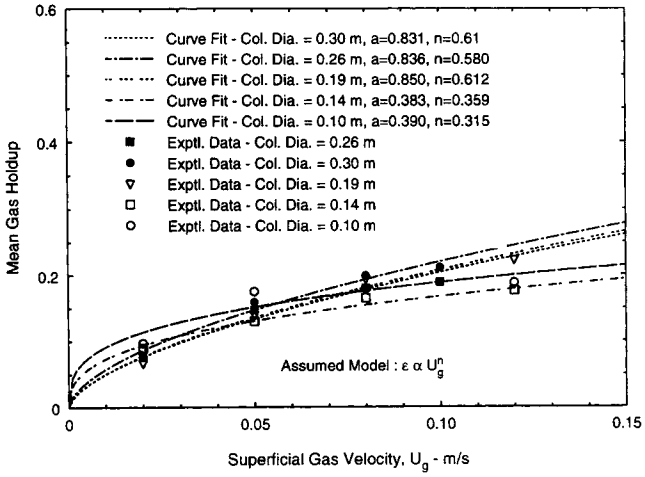

Figure 8. Cross-sectional mean holdup as a function of superficial gas velocity in the columns.

$$\epsilon \propto U_g^n, \tag{5}$$

where n is an exponent typically in the range of 0.6 to 0.8 (Shah et al., 1983). Bach and Pilhofer (1978) have correlated the overall gas holdup measured with a wide range of liquids with the relation

$$\frac{\epsilon}{1-\epsilon} = U_g^{0.7}. \tag{6}$$

The cross-sectional mean holdup in the various columns over the range of superficial gas velocities studied are examined for a similar relationship. Figure 8 shows the experimental data for the gas holdup plotted as a function of superficial gas velocity for all the column diameters studied. Also shown in the plot are the curve fits to the data based on Eq. 5. The exponent n and the constant of proportionality obtained here appear to fall in two classes, with similar values being obtained for columns less than or equal to 0.15 m and greater than 0.15 m in diameter. A universal number for these constants is not obtained, the most probable reason being the differences in the open area of the distributors used in the various columns.

Effect of distributor type

The effect of the type of distributor used on the gas-holdup distribution was studied in .the 0.19-m-diameter column. Three different kinds of distributors were used. The first of these was a perforated plate, the characteristics of which are tabulated in Table 4. The second is a cone distributor, and the third distributor used was a bubble cap. Their geometrical characteristics are illustrated in Figure 9.

The cross-sectional distribution of the holdup shown in Figure 10 clearly shows the differences resulting from the distributors. It is seen that the perforated plate results in a uniform distribution of the gas, and this gets reflected in the gradual variation in the color shades for the gas holdup from the column center to the wall. For the cone and the bubble cap distributors the gas moves up the column as large bubbles in a region close to the column center. The peripheral regions are almost unaerated, and this is reflected as an annulus of lighter colors in the cross-sectional image. At the higher gas velocities these differences get minimized to a large extent, owing to the breakup of the large bubbles due to the higher intensity of turbulence generated at these flow rates.

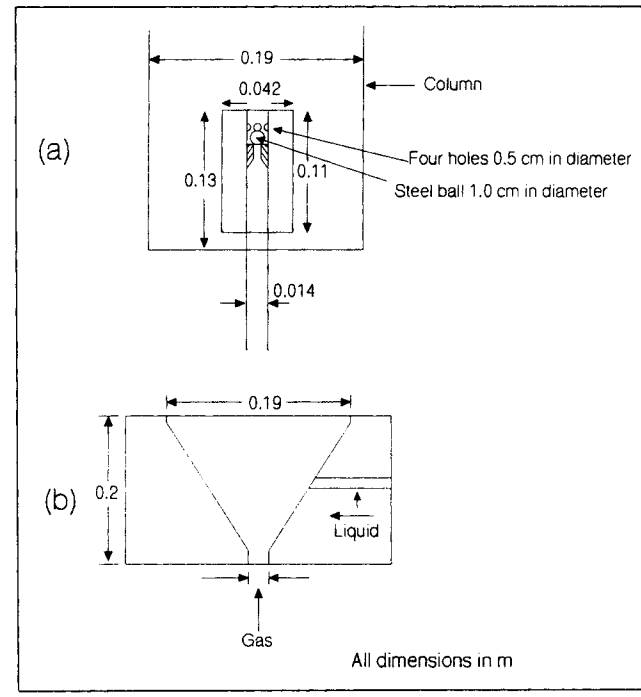

Figure 9. Characteristics of: (a) bubble cap; (b) cone distributor.

It is common in academic research to use a sintered-plate distributor. The difference resulting from the use of such a distributor as against a perforated-plate distributor was studied in the 0.10-m-diameter column. The liquid phase used was a mixture of isopropanol and water mixed in equal volumes. The comparison between the gas-holdup distribution resulting from the two kinds of distributors are shown in Figure 11. This mixture resulted in very fine bubbles, and at high velocities also led to excessive foaming, especially with the sintered-plate distributor. The magnitude of the holdup generated by the sintered plate is larger than that of the perforated plate, and this difference increases with increase in gas velocity.

Effect of static liquid height

Depending on the bubble coalescence and breakup characteristics of the system, the initial liquid height may or may not have a bearing on the gas holdup of the system. In the literature there have been investigations reporting the influence of static liquid height as well as negating any such influence on the holdup. However, it is now generally accepted that for columns with L/D ratios of greater than 5, the gas holdup is independent of this ratio. There have been no reports of the effect of the static liquid height on the local gas holdup and its distribution.

In the present study the influence of the static liquid height on the local gas-holdup distribution was investigated by con-

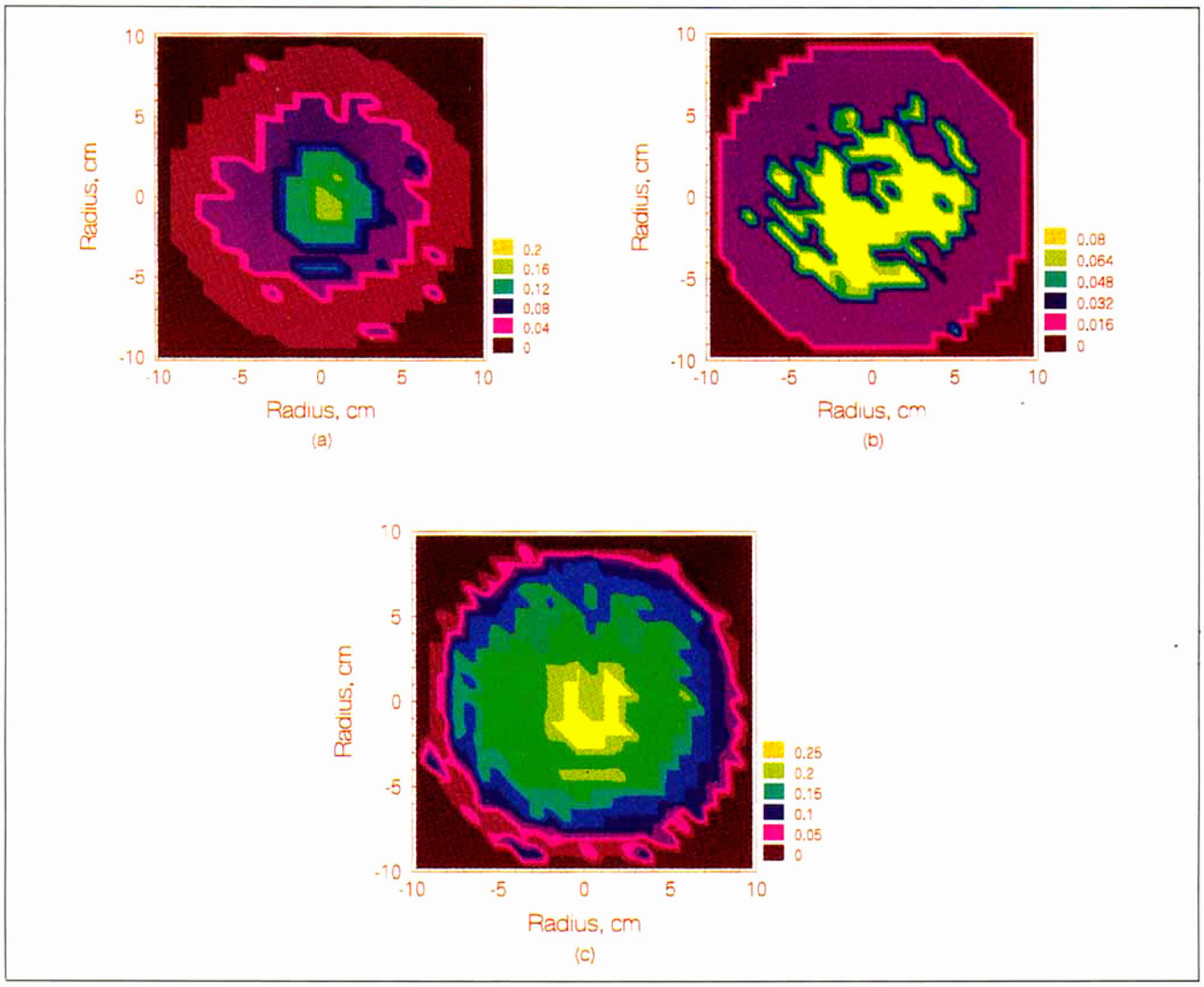

Figure 10. Effect of distributor type on the gas-holdup distribution–air–water system: col. ID = 0.19 m, U_g = 0.05 m/s; (a) bubble cap; (b) cone; (c) perforated plate.

sidering L/D ratios less than 5, equal to 5, and greater than 5. The effect was investigated in two column diameters (0.14 m and 0.30 m) at a low and a high gas superficial velocity. The resulting radial gas-holdup profiles were almost identical with no more than a $\pm 3\%$ difference between the three cases. It was therefore concluded that static liquid height had no effect on radial-holdup distribution or its overall magnitude.

Effect of axial distance from the distributor

For most of the columns studied the tomographic scans were made at five different axial locations above the distributor in order to see the evolution of the gas-holdup distribution with the axial distance from the distributor. Figure 12 depicts the results of this investigation for two different column sizes. In the small column at high gas velocity (Figure 12a) it seems that the middle part of the column has a rather similar gas-holdup radial distribution, with holdup distributions in the entry region and disengagement zone being different as expected. However, at low gas velocity and large column diameter (Figure 12b) an entry region cannot be defined, as the holdup distribution continues to change with increase in axial distance, both in terms of magnitude of the cross-sectional mean as well as in terms of the power-law exponent m. This observation should not be confused with the finding that there was no effect of the L/D ratio on the gas-holdup distribution. The previous result implies that the gas-holdup distribution at any given axial location (away from the distributor and the free surface) depends only on the flow upstream and that it does not matter how far the flow extends beyond that section. On the other hand, the present result implies that the gas-holdup distribution keeps changing with axial distance. The increase in the magnitude of the gas holdup with increasing distance from the distributor could be attributed to the coalescence and breakup characteristics of the bubbles in the system. The initial bubble sizes (formed at the distributor) are probably larger and they gradually break up as they rise up through the column. The smaller bubbles with their reduced velocities lead to an increase in gas holdup with increase in axial distance from the distribu-

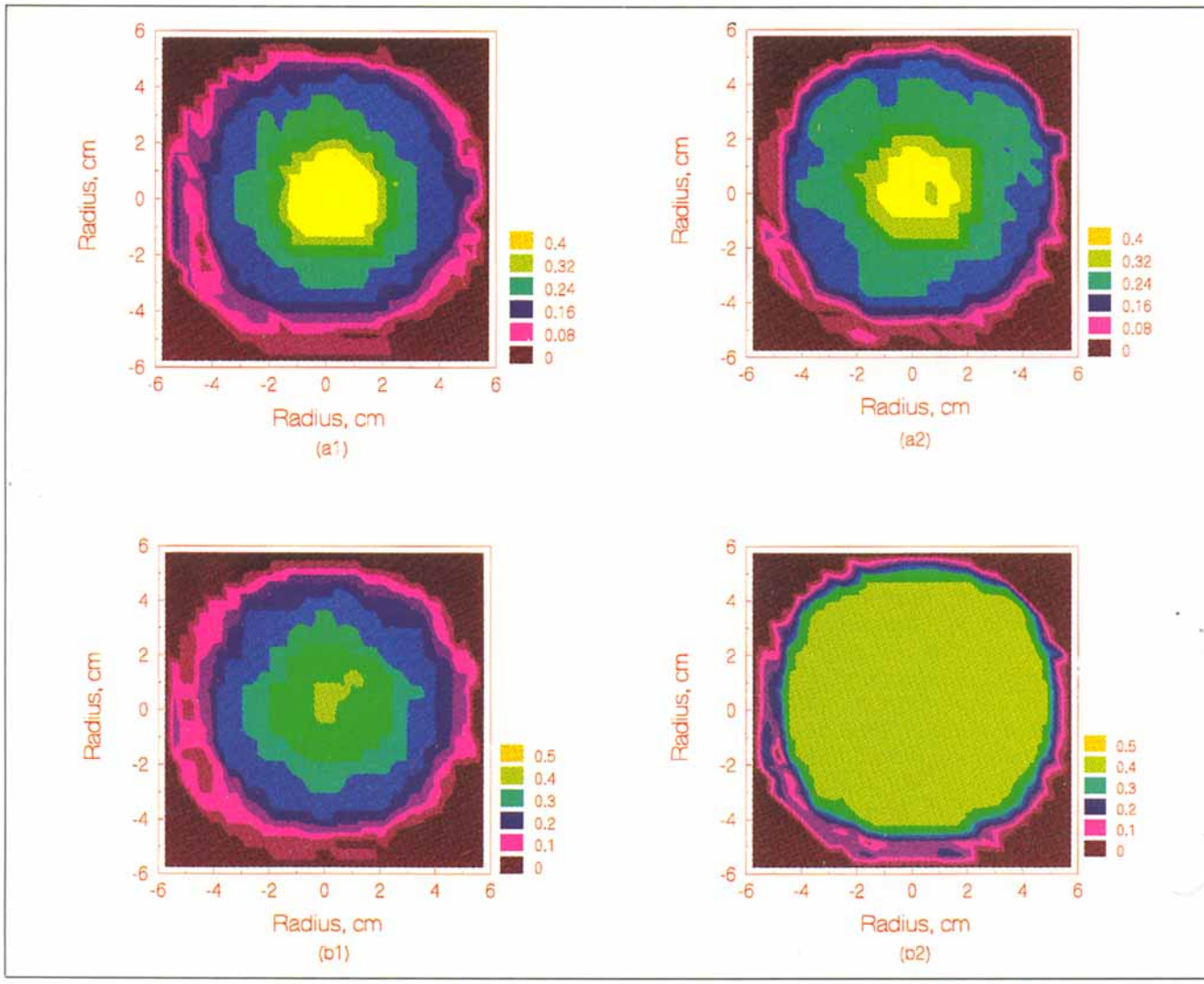

Figure 11. Gas-holdup distribution from sintered-plate and perforated-plate distributor—air–water+alcohol system: col. ID = 0.10 m, $z = 1.0$ m; (a1, a2) $U_g = 0.04$ m/s, (b1, b2) $U_g = 0.08$ m/s; (a1, b1) perforated plate, (a2, b2) sintered plate.

tor. However, the changes in the middle sections of the column (away from the distributor and the free surface) are not too large, even in bubbly flow as can be seen from the cross-sectional mean gas holdup tabulated in Table 8. Consequently, the gas-holdup profile for this central section of the bubble column along the axis can be considered to be a function of the radial coordinate only.

Effect of liquid properties

The effect of using highly purified and deionized water in comparison to regular tap water was studied in the 0.14-m-diameter column. Deionized water was obtained from a compact Milli-Q Plus water-purification system that produces Type I reagent-grade water with a resistivity of 18 MΩ-cm. The column, the distributor, and the plenum were all washed with the same water before the actual runs. The magnitude of the gas holdup and steepness of the profile with the deionized water is always lower than that obtained with regular tap water at all gas velocities. The differences in the magnitude of the gas holdup increased with increasing superficial gas velocity since the bubble sizes increased with increase in the gas flow rate. The maximum difference was observed closer to the center of the column and the magnitude of this difference was about 25%. The bubble sizes observed in the column with deionized water (2 to 3 cm) were much larger in comparison to bubbles of about 0.5 cm in regular tap water. Consequently, the measured holdup with deionized water is lower. These observations are consistent with the results of Anderson and Quinn (1978).

The effect of liquid physical properties was also studied by comparing the gas-holdup distribution obtained with tap water and a mixture of tap water and isopropanol mixed in equal volumes. The mixture had a viscosity of 0.00278 kg/m·s at 26°C, a surface tension of 28.2×10^{-7} N/m and a density of 917 kg/m^3. The bubbles observed in the mixture were small and of the order of 1 to 2 mm. This leads to extremely high values of gas holdup and the comparison between the two

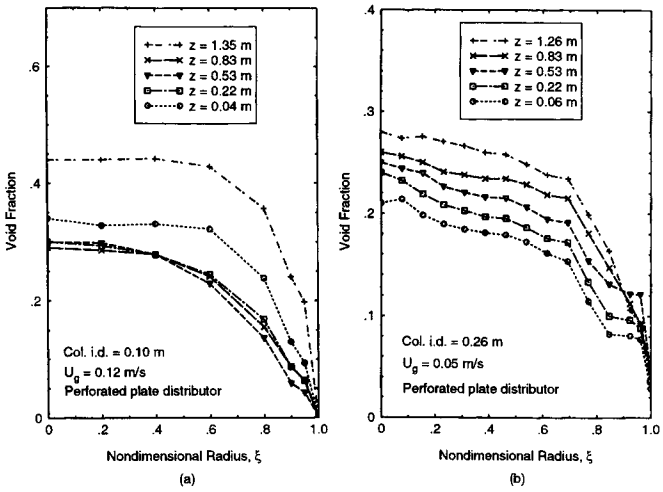

Figure 12. Effect of axial distance on the measured gas-holdup distribution: col. ID (a) 0.10 m; (b) 0.26 m.

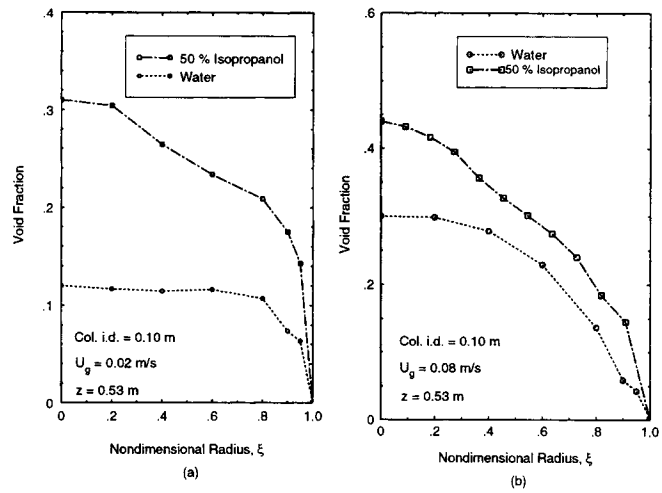

Figure 13. Measured gas-holdup distribution obtained with water and mixture of isopropanol and water: col. ID = 0.10 m; (a) U_g = 0.02 m/s; (b) U_g = 0.08 m/s.

cases is shown in Figure 13. Apparently the dependence of the bubble characteristics as a function of the bubble size is in the regime where the effect of surface tension on bubble sizes and rise velocities is significant (Fan, 1989). At higher gas velocities there is a tendency of the two-phase dispersion to foam with the water–alcohol mixture. It is also interesting to note that owing to their very small size, the bubbles are able to get much closer to the wall, and consequently the gas holdup at the wall is significant. In fact, the gas holdup at the wall for all the runs (not only with the water–alcohol mixture) as obtained with the CT scans is nonzero. Theoretically speaking the gas holdup at the wall should be zero, since there is always a thin layer of the liquid phase on the column wall. Apparently this layer is extremely thin and is not within the spatial resolution capabilities of the scanner.

Significance of Results and Conclusions

From the industrial point of view, the design and scale-up of multiphase flow reactors is of great importance. Any research on the hydrodynamics of such reactors therefore needs to enhance our level of understanding of these complex systems. Since *a priori* solution of multiphase flow problems from a purely theoretical standpoint cannot yet be accomplished, it is necessary to develop models of varying complexity to serve immediate needs. With this phenomenologically oriented approach, experimental data becomes necessary to aid in the development of constitutive equations and correlations for phenomenological and computational fluid dynamic (CFD) models. The use of CFD for multiphase flow modeling is now gaining a lot of attention, and the rigorous documentation of gas holdup and its distribution presented here could serve in benchmarking the numerical simulations.

Thus far results for gas holdup presented in the literature are either qualitative in nature or focused on the overall gas holdup. Qualitative results such as photographs of flow dispersion can only aid in simple analysis such as flow regime determination, and cannot be used in the kind of model-building approach outlined above. Use of overall gas holdup can only suffice in the use of reactor models based on the assumptions of plug flow or completely backmixed (CSTR) reactors or combinations thereof.

The CT scanner has enabled the quantification of the effects of various operating parameters such as the column diameter, the superficial gas velocity, the distributor type and liquid properties on the local gas holdup and its distribution. The common observation that the effect of column diameter on the magnitude of the gas holdup can be neglected, if the diameter is greater than 0.15 m, has been validated. For such columns the assumption of a value of 2 to 2.5 for the power-law exponent for the radial holdup distribution is reasonable. The gas-holdup profiles change from a flatter distribution to a parabolic one, both with increase in column diameter and superficial gas velocity. These profiles continue to change with axial distance from the distributor, and consequently the entrance length required for the profiles to be characterized as fully developed could not be identified. In this sense the flow is truly three-dimensional. However, it appears to be reasonable to assume an average profile based on the gas holdup distribution in sections of the flow away from the end effects. The type of distributor used makes a difference at low gas velocities, and these differences tend to get minimized when the flow gets into the churn-turbulent regime. The nature of the system studied here was such that the bubble properties were affected by the surface tension of the liquid, leading to

Table 8. Cross-Sectional Mean Void Fraction as a Function of Axial Distance

Col. Dia. = 0.1 m, U_g = 0.12 m/s		Col. Dia. = 0.14 m, U_g = 0.092 m/s		Col. Dia. = 0.26 m, U_g = 0.05 m/s	
Z, m	$\bar{\epsilon}$	Z, m	$\bar{\epsilon}$	Z, m	$\bar{\epsilon}$
0.04	0.245	0.045	0.208	0.06	0.132
0.22	0.189	0.22	0.196	0.22	0.148
0.53	0.171	0.60	0.193	0.53	0.170
0.83	0.180	0.83	0.162	0.83	0.183
1.35	0.346	1.19	0.228	1.26	0.198

a profound effect both on the magnitude and shape of the gas-holdup profile. The liquid with lower surface tension produces very fine bubbles and leads to large values of the gas holdup and also to flatter radial holdup profiles. Finally, the versatility of the scanner in measuring the data in a wide range of operating conditions has been demonstrated.

Acknowledgments

The authors are indebted to the industrial participants of the Chemical Reaction Engineering Laboratory (CREL) and to DOE Contract DE FC 22 95 PC 95051 and DOE Grant DE FG 28 95 PC 95212, which provided partial support for this work.

Notation

D = column diameter
g = acceleration due to gravity
L = static liquid height
P = pressure
r = radial position
U_g = gas superficial velocity
Z = axial location
ϵ = local gas holdup
$\bar{\epsilon}$ = cross-sectional mean gas holdup
ρ_l = material density of liquid phase
ξ = nondimensional radius

Literature Cited

Anderson, J. L., and J. A. Quinn, "Bubble Columns: Flow Transitions in the Presence of Trace Contaminants," *Chem. Eng. Sci.*, **25**, 373 (1970).

Bach, H. F., and T. Pilhofer, "Variation of Gas Holdup in Bubble Columns with Physical Properties of Liquids and Operating Parameters of Columns," *Ger. Chem. Eng.*, **1**, 270 (1978).

Clark, K. N., "The Effect of High Pressure and Temperature on Phase Distribution in a Bubble Column," *Chem. Eng. Sci.*, **45**, 2301 (1990).

Dempster, A. P., N. M. Laird, and D. B. Rubin, "Maximum Likelihood Estimates from Incomplete Data via the E-M Algorithm," *J. Royal Statistical Soc.*, **39**, Series B, 1 (1977).

Devanathan, N., D. Moslemian, and M. P. Duduković, "Flow Mapping in Bubble Columns using CARPT," *Chem. Eng. Sci.*, **45**, 2285 (1990).

Fan, L. S., *Gas-Liquid-Solid Fluidization Engineering*, Butterworths, Boston (1989).

Gordon, R., "A Tutorial on ART," *IEEE Trans. Nucl. Sci.*, **NS-21**, 78 (1974).

Herman, G. T., R. M. Lewitt, D. Odhner, and S. W. Rowland, "SNARK89—A Programming System for Image Reconstruction from Projections," Tech. Rep. MIPG160, Univ. of Pennsylvania, Philadelphia (1989).

Hills, J. H., "Radial Non-uniformity of Velocity and Voidage in a Bubble Column," *Trans. Inst. Chem. Eng.*, **52**, 1 (1974).

Huesman, R. H., G. T. Gullberg, W. L. Greenberg, and T. F. Budinger, "Donner Algorithms for Reconstruction Tomography," Lawrence Berkeley Laboratory, Univ. of California, Berkeley (1977).

Kawase, Y., and M. Moo-Young, "Influence of Non-Newtonian Flow Behavior on Mass Transfer in Bubble Columns with and without Draft Tubes," *Chem. Eng. Commun.*, **40**, 67 (1986).

Kelkar, B. G., and Y. T. Shah, "Gas Holdup and Backmixing in Bubble Columns with Polymer Solutions," *AIChE J.*, **31**, 700 (1985).

Kelkar, B. G., S. P. Godbole, M. F. Honath, Y. T. Shah, N. L. Carr, and W. D. Deckwer, "Effect of Addition of Alcohols on Gas Holdup and Backmixing in Bubble Columns," *AIChE J.*, **29**, 361 (1983).

Kovide, K., S. Morooka, K. Veyama, A. Matsura, F. Yamashita, S. Iwamoto, Y. Kato, H. Inoue, M. Shigeta, S. Suzuki and T. Akehata, "Behavior of Bubbles in a Large Scale Bubble Column," *J. Chem. Engg., Japan*, **12**, 98 (1979).

Kumar, B. S., D. Moslemian, and M. P. Duduković, "A γ Ray Tomographic Scanner for Imaging Voidage Distribution in Two-Phase Flow Systems," *Flow Meas. Instrum.*, **6**(3), 61 (1995).

Kumar, B. S., "Computed Tomographic Measurements of Void Fraction and Modeling of the Flow in Bubble Columns," PhD Thesis, Florida Atlantic Univ., Boca Raton (1994).

Lange, K., and R. Carson, "EM Reconstruction Algorithms for Emission and Transmission Tomography," *J. Comp. Assisted Tomog.*, **8**, 306 (1984).

Lewitt, R. M., "Reconstruction Algorithms: Transform Methods," *Proc. IEEE*, **71**, 390 (1976).

Malnes, D., "Slip Ratios and Friction Factors in the Bubble Flow Regime in Vertical Tubes," PhD Thesis, Norwegian Technical Institute, Trondheim (1966).

Moslemian, D., N. Devanathan, and M. P. Duduković, "A Radioactive Particle Tracking Facility for Investigation of Phase Recirculation in Multiphase Systems," *Rev. Sci. Instrum.*, **63**, 4361 (1993).

Miyauchi, T., S. Furusaki, S. Morooka, and Y. Ikeda, "Transport Phenomena and Reaction in Fluidized Catalyst Beds," *Advances in Chemical Engineering*, **11**, 275 (1991).

Newton, T. H., and D. G. Potts, *Radiology of the Skull and Brain*, Vol. 5, *Technical Aspects of Computed Tomography*, Mosby, St. Louis, MO (1981).

Prakash, A., and C. L. Briens, "Porous Gas Distributors in Bubble Columns: Effect of Liquid Presence on Distributor Pressure Drop; Effect of Startup Procedure on Distributor Performance," *Can. J. Chem. Eng.*, **68**, 204 (1990).

Reilly, I. G., D. S. Scott, T. De Bruijn, A. Jain, and J. Piskorz, "A Correlation for Gas Hold-up in Turbulent Coalescing Bubble Columns," *Can. J. Chem. Eng.*, **64**, 1857 (1990).

Serizawa, A., I. Kataoka, and I. Michiyoshi, "Turbulence Structure of Air-Water Bubbly Flow—II Local Properties," *Int. J. Multiphase Flow*, **2**, 235 (1975).

Shah, Y. T., B. G. Kelkar, S. P. Godbole, and W. D. Deckwer, "Design Parameter Estimations for Bubble Column Reactors," *AIChE J.*, **28**, 353 (1982).

Sim, S. K., and R. T. Lahey, Jr., "Measurement of Phase Distribution in a Triangular Duct," *Int. J. Multiphase Flow*, **12**, 405 (1986).

Wang, S. K., S. J. Lee, O. C. Jones, and R. T. Lahey, "3D Turbulence Structure and Phase Distribution Measurements in Bubbly Two Phase Flows," *Int. J. Multiphase Flow*, **13**, 327 (1987).

Wilkinson, P. M., and L. L. V. Dierendock, "Pressure and Gas Density Effects on Bubble Break-up and Gas Holdup in Bubble Columns," *Chem. Eng. Sci.*, **45**, 2309 (1990).

Wilkinson, P. M., A. P. Spek, and L. L. V. Dierendock, "Design Parameter Estimation for Scale-up of High Pressure Bubble Columns," *AIChE J.*, **38**, 544 (1992).

Yamashita, F., "Effect of Liquid Depth, Column Inclination and Baffle Plates on Gas Holdup," *J. Chem. Eng. Japan*, **18**, 349 (1985).

Yang, Y. B., N. Devanathan, and M. P. Duduković, "Liquid Backmixing in Bubble Columns via Computer Automated Radioactive Particle Tracking (CARPT)," *Exp. Fluids*, **16**, 1 (1993).

Yester, M. W., and G. T. Barnes, "Geometrical Limitations of Computed Tomography Scanner Resolution," *Appl. Optical Instrumentation in Medicine*, **127**, 296 (1977).

Manuscript received June 20, 1996, and revision received Jan. 21, 1997.